Canadian Mineralogist
Vol. 18, pp. 443-458 (1980)

FROM UNIT-CELL PARAMETERS TO Si/Al DISTRIBUTION IN K-FELDSPARS

ROBERT B. FERGUSON*
Department of Earth Sciences, University of Manitoba, Winnipeg, Manitoba R3T 2N2

ABSTRACT

Data for the 23 K-feldspars whose structures have now been refined serve to construct curves used to derive the Al contents of the four tetrahedral sites from unit-cell parameters; the data are utilized according to principles different than those used in the Stewart–Wright–Ribbe, Kroll and similar curves. The new curves, applicable to K-feldspars with Or $\geqslant \sim 85$ mol. %, are designed to yield (1) the mean tetrahedral cation–oxygen distance $\overline{T_j\text{–O}}$ (Å) for each T_j site and (2) the corresponding Al content t_j (atomic %), utilizing in effect either of two commonly used t *versus* $\overline{T\text{–O}}$ linear relationships, a "modified Jones–Ribbe–Gibbs" (J–R–G) relationship (Si–O 1.604, Al–O 1.759 Å) and a "modified Smith–Bailey" (S–B) relationship (1.609, 1.745 Å). The curves consist in linear regression lines through plots of observed distances $\overline{T_1\text{–O}}$ and $\overline{T_2\text{–O}}$ (Å) against cell parameters b, c (Å) and c^*/b^* ($=6d_{060}/2d_{002}$) for monoclinic K-feldspars (sanidines, orthoclases, adularias), and through plots of observed distances $\overline{T_1\text{O–O}}$, $\overline{T_1m\text{–O}}$ and the mean of $\overline{T_2\text{O–O}}$ and $\overline{T_2m\text{–O}}$ (Å) against interaxial angle γ (°) for triclinic K-feldspars (microclines). Scales for t assumming each of the J–R–G and S–B t *versus* $\overline{T\text{–O}}$ relationships are added in diagrams for both the monoclinic and the triclinic cases, and scales for γ^* (°) and triclinicity Δ (Goldsmith & Laves 1954) are added parallel to the γ scale in the microcline diagram. The errors in derived results are estimated to be in most cases $\pm$ 0.003 Å in $\overline{T_j\text{–O}}$ and $\pm$ 3 Al (in atomic %) in t_j for a given pair of t and $\overline{T\text{–O}}$ values. The diagrams show that a completely Si/Al disordered (high) sanidine would have $b = 13.047$, $c = 7.171$ Å and that the triclinic microcline series can be interpreted as having a monoclinic end-member with $\overline{T_1\text{–O}}$ and $\overline{T_2\text{–O}}$ equal to 1.660 and 1.624 Å, and t_1 and t_2 equal to $\sim$ 36 and 14% Al, which correspond to the values for orthoclase.

Keywords: feldspar, K-feldspar, Si/Al distributions, tetrahedral Al contents, sanidines, orthoclases, microclines.

SOMMAIRE

Au moyen des données provenant des 23 feldspaths à structure affinée connue, on a construit des courbes destinées à établir, en fonction des paramètres réticulaires, la distribution de l'aluminium sur les quatre sites tétraèdriques d'un feldspath potassique (Or $\geqslant \sim 85$ % mol.). Les principes sur lesquels sont fondées ces courbes diffèrent à ceux qui ont servi à définir les courbes de Stewart–Wright–Ribbe, Kroll et autres. Les nouvelles fonctions sont conçues pour donner (1) la distance moyenne cation–oxygène dans le tétraèdre ($\overline{T_j\text{–O}}$, en Å) pour chaque site T_j et (2) la proportion d'aluminium correspondante t_j (en %) par l'une ou l'autre des relations linéaires entre t et $\overline{T\text{–O}}$ d'usage courant, à savoir: les relations modifiées de Jones–Ribbe–Gibbs (J–R–G: Si–O 1.604, Al–O 1.759 Å) et de Smith–Bailey (S–B: 1.609, 1.745 Å). Ce sont des droites calculées par régression linéaire des distances observées $\overline{T_1\text{–O}}$ et $\overline{T_2\text{–O}}$ (en Å) en fonction des paramètres b, c (en Å) et c^*/b^* ($= 6d_{060}/2d_{002}$) pour les feldspaths monocliniques (sanidines, orthoses, adulaires), et des distances $\overline{T_1\text{O–O}}$, $\overline{T_1m\text{–O}}$ et la moyenne de $\overline{T_2\text{O–O}}$ et $\overline{T_2m\text{–O}}$ en fonction de l'angle γ (°) pour les feldspaths tricliniques (microclines). Pour les feldspaths monocliniques et tricliniques, on a calculé l'échelle de t pour chacune des deux fonctions t de $\overline{T\text{–O}}$; pour les microclines, on a ajouté l'échelle de γ^* (°) et celle de la triclinicité Δ (Goldsmith & Laves 1954) parallèlement à l'axe des γ du diagramme. Dans la plupart des cas, les erreurs dans les quantités dérivées seraient de $\pm$ 0.003 Å sur $\overline{T_j\text{–O}}$ et de $\pm$ 3 Al (%, at.) sur t_j pour chaque paire de valeurs t et $\overline{T\text{–O}}$. D'après nos diagrammes, une sanidine complètement désordonnée aurait $b = 13.047$, $c = 7.171$ Å, et la série de microclines (tricliniques) pourrait avoir un pôle monoclinique où $\overline{T_1\text{–O}}$, $\overline{T_2\text{–O}}$ sont égales à 1.660, 1.624 Å et t_1, t_2, à $\sim$ 36, 14% Al, valeurs correspondant à celles de l'orthose.

(Traduit par la Rédaction)

Mots-clés: feldspath, feldspath potassique, distribution de Si et de Al, cations tétraédriques, sanidine, orthose, microcline.

INTRODUCTION

The method of Stewart & Ribbe (1969) and

*The work described here was done in the Department of Geology and Mineralogy, The University of Adelaide, Adelaide, South Australia, during a sabbatical leave in 1979-80.

Stewart & Wright (1974) for rapidly deriving the Si/Al distributions (tetrahedral Al contents) in alkali feldspars from unit-cell parameters is in common use to structurally characterize individual potassium feldspars (sanidines, orthoclases, microclines) or sodium feldspars (albites) in granitic and related rocks in order to obtain petrogenetic interpretations. Somewhat similar to the Stewart-Wright-Ribbe determinative method is the procedure of Kroll (1973) which has, however, received little attention. Others have described closely related methods (*e.g.*, Smith 1974, Hovis 1974, Blasi & Blasi De Pol 1977), but the principles are basically the same; the Stewart–Wright–Ribbe and Kroll methods can be regarded as the prototypes.

These determinative methods are based on the assumption that one or more of the unit-cell parameters (a, b, c, α, β, γ) or the corresponding reciprocal cell parameters (a^*, b^*, c^*, α^*, β^*, γ^*) varies perceptibly and regularly with change in the Si/Al distribution (expressed as atomic % Al statistically occupying a given tetrahedral site). The correlations of Al content with unit-cell parameter (usually expressed graphically) ultimately are based on information derived from detailed structure analyses of relevant feldspars utilizing X-ray diffraction or,

TABLE 1. UNIT CELL PARAMETERS (Å,°), $\overline{T_j\text{-}O}$ DISTANCES (Å) AND TETRAHEDRAL Al-CONTENTS t_j (%) OF STRUCTURALLY REFINED K FELDSPARS†

Sample#	a	b	c	Tr[110] Tr[1$\bar{1}$0]	α α*	β	c* b*	γ γ*	$\overline{T_j\text{-}O}$ distances T_1 T_1^0 T_1^m	 T_2 T_2^0 T_2^m	Al contents t_1 t_1^0 t_1^m	 t_2 t_2^0 t_2^m	 Σ+	 t_1 t_1^0 t_1^m	 t_2 t_2^0 t_2^m	 Σ++	Ref.##
Monoclinic: space group C2/m																	
(1)	8.546(5)	13.037(5)	7.178(5)	15.588(7)	-	115.97(5)	2.0202(4)		1.645(2)	1.641(2)	26	24	100	26	24	100	(1)
(2)	8.5642(2)	13.0300(4)	7.1749(2)	15.593(4)	-	115.994(5)	2.02044(3)		1.645[2]	1.640[2]	26	23	98	26	23	98	(2,3,4)
(3)	8.539(4)	13.015(5)	7.179(3)	15.566(6)	-	115.99(2)	2.0169(3)		1.650[1]	1.637[1]	30	21	102	30	21	102	(5)
(4)	8.552(6)	13.030(9)	7.179(6)	15.586(11)	-	115.91[5]	2.0178(6)		1.650(1)	1.635(1)	30	20	100	30	19	98	(6)
(5)	8.549(5)	13.028(5)	7.188(5)	15.582(7)	-	116.02(5)	2.0169(4)		1.653(2)	1.635(2)	32	20	104	32	19	102	(1)
(6)	8.575(2)	13.007(3)	7.191(2)	15.579(4)	-	115.977(20)	2.0121(2)		1.654[1]	1.634[1]	32	19	102	33	18	102	(7)
(7)	8.561(2)	12.996(4)	7.192(2)	15.562(4)	-	116.01(1)	2.0107(2)		1.656(3)	1.628(3)	34	15	98	35	14	98	(3,4,8)
(8)	8.554(2)	12.970(4)	7.207(2)	15.537(4)	-	116.007(10)	2.0024(2)		1.664(2)	1.622(2)	39	12	102	40	10	100	(4)
(9)	8.545(2)	12.967(5)	7.201(3)	15.529(5)	-	116.00(2)	2.0035(3)		1.665[1]	1.621[1]	39	11	100	41	9	100	(5)
(10)	8.5632(11)	12.963(14)	7.2099(11)	15.536(18)	-	116.073(9)	2.0016(4)		1.667(1)	1.616(1)	41	8	98	43	5	96	(9)
††Metrically monoclinic, structurally triclinic: space group C$\bar{1}$																	
(11)	8.589(2)	13.013(7)	7.197(2)	15.592(7)	-	116.02(3)	2.0121(12)		1.660[1] 1.657[1]	1.631[1] 1.630[1]	36 34	17 17	104	38 35	16 15	104	(10)
(12)	8.583(2)	12.988(7)	7.202(2)	15.568(7)	-	116.05(3)	2.0073(12)		1.665[1] 1.655[1]	1.626[1] 1.626[1]	39 33	14 14	100	41 34	13 13	101	(10)
(13)	8.563(2)	12.990(7)	7.210(2)	15.558(7)	-	115.93(3)	2.0033(12)		1.672[1] 1.659[1]	1.623[1] 1.623[1]	44 35	12 12	103	46 37	10 10	103	(10)
Triclinic: space group C$\bar{1}$																	
(14)	8.567(2)	12.980(7)	7.200(2)	15.590(7) 15.515(7)	90.18(3) 90.05(3)	116.03(3)	89.70(3) 90.25(3)		1.669[1] 1.654[1]	1.623[1] 1.622[1]	42 32	12 12	98	44 33	10 10	97	(10)
(15)	8.643(3)	12.929(4)	7.190(3)	15.602(5) 15.502(5)	90.13(3) 90.05[3]	116.24(3)	89.60(3) 90.38[3]		1.671(3) 1.651(3)	1.622(3) 1.627(3)	43 30	12 15	100	46 31	10 13	100	(11,12)
(16)	8.564(2)	12.984(7)	7.201(2)	15.620(7) 15.488(7)	90.30(3) 90.08(3)	116.02(3)	89.47(3) 90.45(3)		1.674[1] 1.651[1]	1.624[1] 1.621[1]	45 30	13 11	99	48 31	11 9	99	(10)
(17)	8.5784[14]	12.9600[10]	7.2112[12]	15.651[1] 15.432[1]	90.30[3] 90.10[3]	116.03[3]	89.12[3] 90.83[3]		1.694[3] 1.643[3]	1.619[3] 1.616[3]	58 25	10 8	101	63 25	7 5	100	(13,14)
(18)	8.560(2)	12.984(7)	7.209(2)	15.691(7) 15.411(7)	90.62(3) 90.15(3)	116.03(3)	88.88(3) 90.93(3)		1.694[1] 1.643[1]	1.620[1] 1.619[1]	58 25	10 10	103	63 25	8 7	103	(10)
(19)	8.574(2)	12.962(7)	7.210(2)	15.715(7) 15.365(7)	90.80(3) 90.20(3)	116.03(3)	88.60(3) 91.17(3)		1.701[2] 1.631[2]	1.620[2] 1.619[2]	63 17	10 10	100	68 16	8 7	99	(10)
(20)	8.567(2)	12.970(7)	7.221(2)	15.763(7) 15.322(7)	91.00(3) 90.25(3)	116.00(3)	88.23(3) 91.47(3)		1.717[1] 1.630[1]	1.615[1] 1.615[1]	73 17	7 7	104	79 15	4 4	102	(10)
(21)	8.561(2)	12.972(7)	7.223(2)	15.845(7) 15.234(7)	91.42(3) 90.38(3)	115.97(3)	87.55(3) 92.03(3)		1.731[1] 1.618[1]	1.616[1] 1.616[1]	82 9	8 8	107	90 7	5 5	107	(10)
(22)	8.5726[16]	12.9618[18]	7.2188[18]	15.818[2] 15.257[2]	90.57[3] 90.47[3]	115.92[3]	87.75[3] 92.22[3]		1.735(6) 1.613(6)	1.619(6) 1.609(6)	85 6	10 3	104	93 3	7 0	103	(15)
(23)	8.560(4)	12.964(7)	7.215(3)	15.819(8) 15.246(8)	90.65(8) 90.38(8)	115.83(8)	87.70(8) 92.23(8)		1.741(5) 1.614(5)	1.611(5) 1.612(5)	88 6	5 5	104	97 4	1 2	104	(16)

+ and ++ calculated from 'modified Jones-Ribbe-Gibbs' and 'modified Smith-Bailey' curves respectively. Σ = sum of tetrahedral populations.

(1) Heated sanidine (2) Heated Spencer C orthoclase (3) Low sanidine #7002 (4) Sanidine #7002 (5) Sanidine (6) Adularia, St.Gotthard #297 (7) Spencer C orthoclase (8) Spencer B adularia (9) Adularia #7007 (10) Ordered orthoclase (11) P2B (12) P2A (13) CA1A (14) P17C (15) K235 (16) A1D (17) Spencer U (18) CA1B (19) P1C (20) RC20C (21) CA1E (22) Pontiskalk (23) Pellotsalo

##(1) Weitz 1972 (2) Ribbe 1963 (3) Cole *et al.* 1949 (4) Colville & Ribbe 1968 (5) Phillips & Ribbe 1973 (6) Brown *et al.* 1974 (7) J.B. Jones, pers. comm. 1979 (8) Jones & Taylor 1961 (9) Prince *et al.* 1973 (10) Dal Negro *et al.* 1978 (11) Ribbe 1979 (12) Ribbe & Gibbs 1975 (13) Bailey 1969 (14) Bailey & Taylor 1955 (15) Finney & Bailey 1964 (16) Brown & Bailey 1964

† Standard deviations enclosed in [ ] were assigned in this study. †† For this group, γ = γ* = 90.00(3)° for all samples.

in a few cases, neutron diffraction.

Since publication of the Stewart–Wright–Ribbe and Kroll determinative curves, many more alkali feldspar structures, in particular of K-rich feldspar, have been refined. It is now possible to assess these two prototype determinative methods and to establish new and more direct tetrahedral Al-content determinative curves for sanidines, orthoclases and microclines.

Sources of Data

Data for fewer than the 13 K-feldspars refined by 1974 were utilized by Stewart & Wright (1974) and Kroll (1973); at present, data are available for 23 refined K-feldspar structures, 10 of which are monoclinic (sanidines, orthoclases and adularias) and 13 triclinic (microclines), including 3 that are geometrically monoclinic. Table 1 gives the relevant data for these 23 K-feldspars. The original authors' papers show that these feldspars have compositions with Or $\geqslant \sim 85$ mole %; all discussion and conclusions thus apply strictly only to K-feldspars within the composition range Or_{85} to Or_{100}.

Assessment of the Stewart–Wright–Ribbe and Kroll Determinative Methods

The Stewart–Wright–Ribbe (S–W–R) method

This procedure, described by Stewart & Ribbe (1969) and Stewart & Wright (1974), is based closely on work by Orville (1967) and Wright & Stewart (1968). Smith (1974, chapter 7) has assessed Stewart's & Ribbe's (1969) description of the method, and Stewart (1975) and Ribbe (1975) have made further comments on their approach.

Several characteristics of this method have a bearing on the choice of presentation of the new determinative diagrams described below. (The notation used in these methods is described in the accompanying Glossary.) The first characteristic relates to the nature of the variables used in the S–W–R determinative diagrams. For the alkali feldspars, their diagrams show the variations in certain sums and differences of the Al contents in the possible tetrahedral sites, with variation in certain direct and reciprocal cell parameters: a plot of direct cell parameters b against c (Å) is contoured to yield the Al-content sums $t_1O + t_1m$ in microclines and albites (triclinic), or $2t_1$ (atomic %) in orthoclases and sanidines (monoclinic); in addition, for the triclinic members a plot of reciprocal

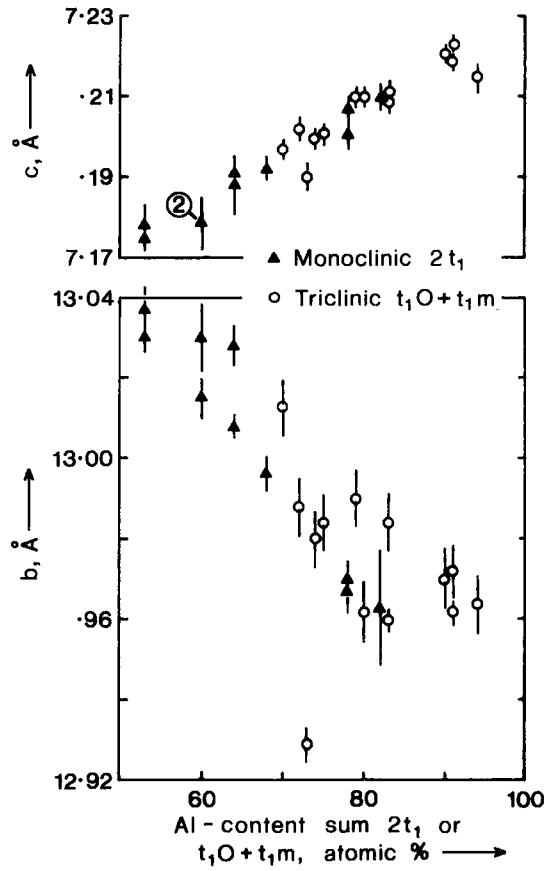

FIG. 1. Plots of b and c (Å) against the Al-content sum (monoclinic) $2t_1$ or (triclinic) $t_1O + t_1m$ (atomic %) for the 23 K-feldspars whose structures have been refined. Data from Table 1. Al contents t_j are those based on the modified Jones–Ribbe–Gibbs (J–R–G) t *versus* $\overline{T\text{–}O}$ relationship. Error bars are shown for b and c; because of the assumptions involved in deriving t_j values, errors in the abscissa units were not deduced. The significance of the plots is discussed in the text.

cell angles α^* against γ^* (°) is contoured to yield t_1O–t_1m. This sum yields t_1 for a monoclinic alkali feldspar or, combined with t_1O–t_1m, t_1O and t_1m for a triclinic member. The Al-content sums $2t_2$ in the other pair of equivalent monoclinic sites T_2, or t_2O+t_2m in the remaining two triclinic sites T_2O, T_2m are obtained by difference (for total Al = 100%); the individual values of t_2 or of t_2O, t_2m are obtained from the fact that any pair of such monoclinic sites must have (or of triclinic sites is assumed to have) equal Al contents, *i.e.*, $t_2O = t_2m$.

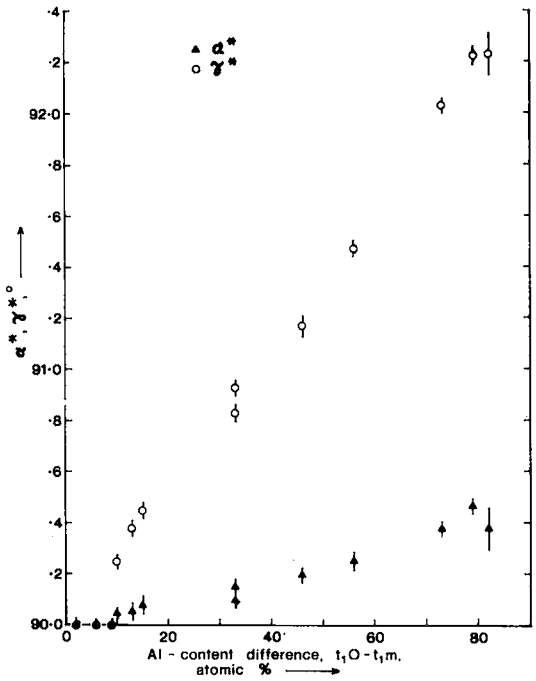

FIG. 2. Plots of α^* and γ^* (°) against the Al-content difference t_1O–t_1m (atomic %) for the 13 triclinic K-rich feldspars (microclines) whose structures have been refined. Data from Table 1. Al contents t_j are those based on the modified Jones–Ribbe–Gibbs (J–R–G) *t versus* $\overline{T\text{–}O}$ relationship. Error bars are shown for α^* and γ^*; because of the assumptions involved in deriving t_j values, errors in t_1O–t_1m were not deduced. The significance of the plots is discussed in the text.

The *b*–*c* plot is also contoured for *a*, which is sensitive to be ratio K/(K+Na) in an alkali feldspar and which Stewart & Wright (1974) used to derive an "index of strain $\triangle$"; this aspect is not of concern here.

This method thus assumes that the sums $t_1O + t_1m$ or $2t_1$ are measurable functions of *b* and *c*, and that the differences t_1O–t_1m are such functions of α^* and γ^*. Although Stewart & Ribbe (1969) and Blasi (1978) have offered structural explanations for the variations of *b*–*c* and α^*–γ^*, respectively, with changing Si/Al distributions, a plot of these unit-cell parameters against the Al-content sums or differences for refined structures has not been published. The data from Table 1 have been used to plot *b* and *c* against $t_1O + t_1m$ and t_2 in Figure 1, and (triclinic) α^* and γ^* against t_1O–t_1m in Figure 2. It may be seen from these two figures that *b* and *c* do vary measurably with $t_1O + t_1m$ or $2t_1$ and α^* and γ^* with t_1O–t_1m, as the method assumes; the plots also emphasize that there would be appreciable error in a derived value of $t_1O + t_1m$ or t_2 due to the scatter of the plotted points (greater for *b* than for *c*), and in a derived value of t_1O–t_1m, particularly from α^* because of the insensitivity of t_1O–t_1m with respect to α^*.

Because the deduced individual Al contents t_1 and t_2 (monoclinic) or t_1O, t_1m and $t_2O = t_2m$ (triclinic) result from the use of two cell parameters (*b*, *c*) in the monoclinic case and of four parameters (*b*, *c*, α^*, γ^*) in the triclinic case, and because of the scatter in the plots and the insensitivity of some of the relationships between Al content and cell parameter, a substantial error would be introduced into t_j values derived by this means. A plot that is likely to lead to more precise tetrahedral Al contents is one that utilizes one or two of the most sensitive unit-cell parameters to yield *individual* values of t_j rather than sums or differences of two t_js. The new determinative diagrams described below utilize in effect one sensitive determinative parameter each for the monoclinic and triclinic groups of K-feldspars.

The second characteristic of the S–W–R method that has a bearing on the new curves relates to the amount of structural data used in the preparation of the determinative diagrams. In constructing their *b*–*c* and α^*–γ^* plots, the authors utilized refined structural data for only the four end-members that define their quadrilaterals: maximum microcline, (high) sanidine, analbite (high albite) and low albite. The new determinative diagrams make use of the relevant data for the 10 monoclinic and the 10 structurally and geometrically triclinic K-feldspars whose structures have now been refined.

The third characteristic of this method that is relevant to the new curves concerns the fact that the authors' determinative diagrams yield directly the Al contents t_j that embody a subjective element, namely, an implied particular relationship between Al content *t* and mean tetrahedral cation–oxygen distance $\overline{T\text{–}O}$. Furthermore, the two ordered end-members of their quadrilaterals, maximum microcline and low albite, are assumed to be fully Si/Al ordered (t_1O = 100% Al) even though Table 1 in Stewart & Ribbe (1969) shows maxima of only ~ 89% Al in both the maximum microcline and the low albite structures. The matter of the *t versus* $\overline{T\text{–}O}$ relationship is dealt with below, but it may be noted here that the new curves

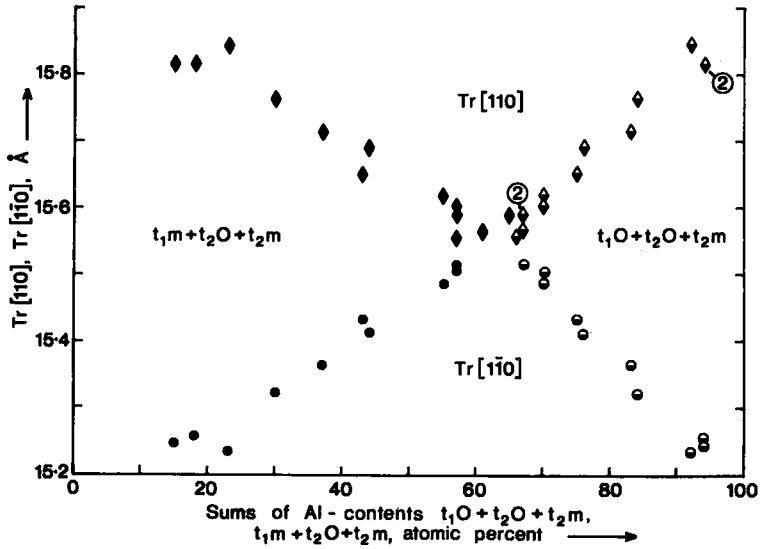

FIG. 3. Plots of Tr[110] (diamonds) and Tr[1$\bar{1}$0] (circles) (Å) against the sums of the Al contents $t_1O + t_2O + t_2m$ (half-solid symbols) and $t_1m + t_2O + t_2m$ (solid symbols) (atomic %) in the manner of Kroll (1973) for the 13 triclinic K-feldspars (microclines) whose structures have been refined. Data from Table 1. The Al contents are those based on the modified Jones–Ribbe–Gibbs (J–R–G) t *versus* $\overline{T\text{–}O}$ relationship, and they have been normalized to $\Sigma\, t_j$ ($=\Sigma$ Al) $= 100\%$. Error bars are not shown because errors in the Tr units are too small to plot on the scale of the diagram, and errors in the t_j sums were not deduced because of the assumptions involved. The diagram corresponds to the right-hand one in Figure 2 of Kroll (1973) except for the omission of the data for monoclinic specimens (see text) and the addition of the plots for Tr[110] versus $t_1m + t_2O + t_2m$ and for Tr[1$\bar{1}$0] *versus* $t_1O + t_2O + t_2m$. The significance of the plots is discussed in the text.

allow for different possible t *versus* $\overline{T\text{–}O}$ relationships and make no *a priori* assumption about the extent of the Si/Al ordering in maximum microcline.

The Kroll method

The method of Kroll (1973; see also Kroll 1980) utilizies Tr[110] and Tr[1$\bar{1}$0] (see Glossary) as determinative parameters to obtain (triclinic case) $t_1O + t_2O + t_2m$ and $t_1m + t_2O + t_2m$, respectively, from which, assuming $\sum_{j=1}^{4} t_j = 100\%$ and $t_2O = t_2m$, the values of the individual Al contents t_1O, t_1m and $t_2O = t_2m$ are obtained. For monoclinic structures for which Tr[110] $= Tr$[1$\bar{1}$0] and $t_1O = t_1m = t_1$ and $t_2O = t_2m = t_2$, the variation in Tr[110] is, as Kroll points out, too small to be suitable for determinative purposes; his method is thus applicable only to triclinic alkali feldspars. As in the S–W–R method, the Kroll method assumes that maximum microcline and low albite are fully Si/Al ordered.

Plots corresponding to Kroll's, using the structural data given in Table 1 for the 13 microclines now refined, are shown in Figure 3, which also includes plots not given by Kroll, namely, of Tr[110] against $t_1m + t_2O + t_2m$, and of Tr[1$\bar{1}$0] against $t_1O + t_2O + t_2m$. It can be seen from this figure that Tr[110] and Tr[1$\bar{1}$0] are valid determinative parameters for deriving t_1O, t_1m and $t_2O = t_2m$ in microclines. However, Tr[110] and Tr[1$\bar{1}$0] are functions of the interaxial angle γ (as well as periods a and b); since it can be shown that γ is the most sensitive of the unit-cell parameters to gauge the triclinic character and hence to infer the Si/Al distribution in a microcline, the present author has utilized the angle γ in the new determinative curves for microclines to derive individual Al contents t_j.

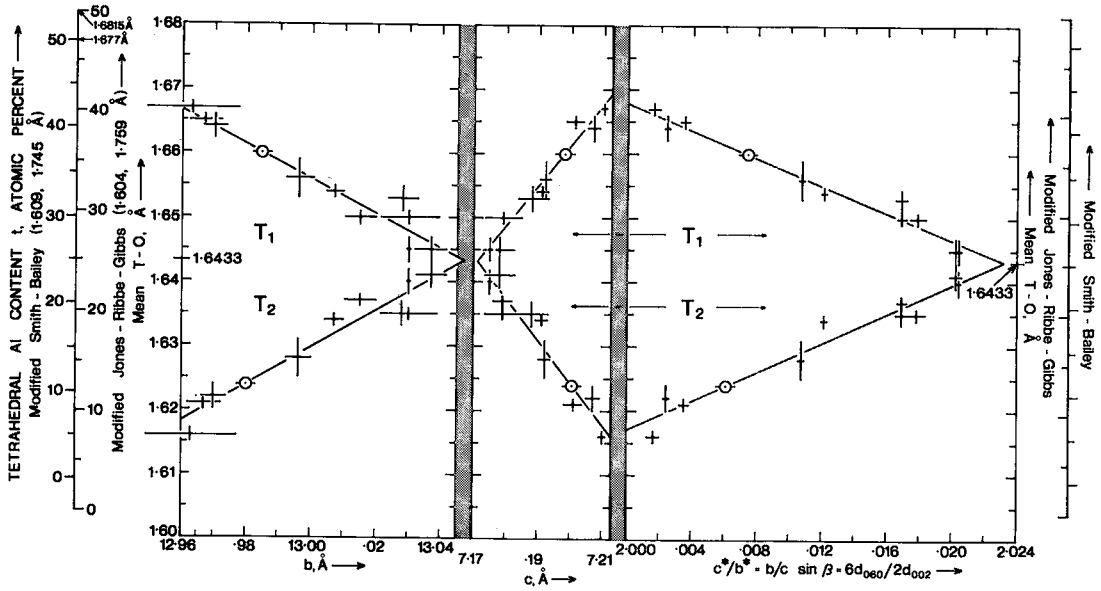

FIG. 4. Determinative diagram for sanidines, orthoclases and adularias; plots with linear regression lines of the observed mean tetrahedral distances $\overline{T_1\text{–O}}$ and $\overline{T_2\text{–O}}$ (Å) against b (Å), c (Å) and c^*/b^* for the 10 monoclinic K-feldspars whose structures have been refined. Data from Table 1. Bar lengths indicate standard deviations or errors. Additional ordinate scales are provided to read tetrahedral Al contents t_j (atomic %) assuming both the "modified Jones–Ribbe–Gibbs" (J–R–G) and the "modified Smith–Bailey" (S–B) t *versus* $\overline{T\text{–O}}$ relationships described in the text. Equations for the regression lines are given in Table 2. The points plotted as circles and the diagram as a whole are discussed in the text.

THE NEW DETERMINATIVE METHOD

Principles

In the foregoing discussion the author has referred to some of the principles embodied in the new determinative curves for K-feldspars. These principles are explained below, and reference is made to the new determinative diagrams shown as Figures 4 and 5 even though the full description of these figures is left until later. *Principle* (1) The relevant data for all the refined K-feldspars presently available (Table 1) should be used in the construction of the determinative diagrams. *Principle* (2) Because tetrahedral Al contents t_j deduced from unit-cell parameters embody a relationship between mean tetrahedral cation–oxygen distance $\overline{T\text{–O}}$ (Å) and the Al content t (%), and because two different t *versus* $\overline{T\text{–O}}$ relationships are in general use today, it is desirable to relate the determinative cell parameter(s) first to objective $\overline{T_j\text{–O}}$ values and second to t_j values utilizing one or more chosen t *versus* $\overline{T\text{–O}}$ relationships. The new determinative curves (Figs. 4, 5) have been constructed in this way. *Principle* (3a) A minimum number of the cell parameters most sensitive to changes in $\overline{T\text{–O}}$ and t should be utilized in order to minimize the error in the derived values of $\overline{T_j\text{–O}}$ and t_j. (b) Different parameter(s) should be used for the monoclinic and triclinic members if this appears desirable. (c) The diagrams should be designed to yield individual values of ($\overline{T_j\text{–O}}$ and) t_j, *i.e.*, t_1, t_1O, t_1m, *etc.*, rather than sums or differences of t_js, *i.e.*, t_1O + t_1m, t_1m + t_2O + t_2m (impossible in terms of $\overline{T_j\text{–O}}$ in any event), again to minimize the error in the derived values.

As in the case of the first two principles, it has been possible, as described below, to utilize these three related principles in deriving the new correlations.

The relationships between Al-content t and $\overline{T\text{–O}}$ distance

As the discussion of principle 2 in the preceding section indicates, the use of determinative diagrams of the types dealt with in this paper involves, explicitly or implicitly, two steps: (1) the derivation from selected cell parameters of

$\overline{T_j\text{–O}}$ distances that are geometrical and require no judgement on the part of the observer, and (2) an inference of the Al contents t_j from some *t versus* $\overline{T\text{–O}}$ relationship that the observer adopts, consciously or unconsciously. The S–W–R, Kroll and most other similar methods incorporate in their determinative diagrams or equations the widely used *t versus* $\overline{T\text{–O}}$ relationship of Ribbe & Gibbs (1969) and Ribbe *et al.* (1974), which assumes a linear relationship between Si–O = 1.605 Å and Al–O = 1.757 Å; these are close to the values 1.603 Å and 1.761 Å, respectively, adopted earlier by Jones (1968). However, another appreciably different linear (or bilinear) relationship of *t versus* $\overline{T\text{–O}}$ also in use is that of Smith & Bailey (1963), who proposed Si–O = 1.61, Al–O = 1.75 Å, and Smith (1974, p. 70), who modified these to Si–O = 1.612, $Si_{½}Al_{½}$–O = 1.676, Al–O = 1.745 Å.

It is because these two *t versus* $\overline{T\text{–O}}$ relationships, the Jones–Ribbe–Gibbs and the Smith–Bailey, are both being used today and also because they lead to significantly different tetrahedral Al contents, especially for the more ordered members (Table 1), that the writer has incorporated both relationships (slightly modified) into the new curves described here.

Both *t versus* $\overline{T\text{–O}}$ relationships adopted here are taken as (uni)linear between Si–O and Al–O, *i.e.*, between $t = 0$ and 100% Al, and both have been chosen such that for $t = 25\%$ Al, $Si_{¾}Al_{¼}$–O = 1.643 Å, the grand mean distance of all the tetrahedra in the 23 K-feldspars now refined (Table 1). The first of the adopted relationships assumes for Si–O ($t = 0\%$ Al) and Al–O ($t = 100\%$ Al) tetrahedral distance values that are simply the means of those (given above) proposed by Jones (1968) on the one hand, and Ribbe & Gibbs (1969) and Ribbe *et al.* (1974) on the other. In the modified Jones–Ribbe–Gibbs (J–R–G) relationship, Si–O = 1.604 Å, Al–O = 1.759 Å.

The second relationship adopted assumes Si–O and Al–O values as close as possible to those proposed by Smith & Bailey (1963) and Smith (1974, p. 70), as given above, but modified (1) to be unilinear rather than bilinear (the latter being unjustified, in the author's opinion, in view of the experimental error in the use of the relationship); (2) to incorporate $Si_{¾}Al_{¼}$–O = 1.643 Å; and (3) to ensure that Si–O is not larger than the minimum $\overline{T\text{–O}}$ yet observed in a K-feldspar structure, 1.609 Å (Table 1). In the modified Smith–Bailey (S–B) relationship, Si–O = 1.609 Å, Al–O = 1.745 Å.

It is the J–R–G and the S–B *t versus* $\overline{T\text{–O}}$ relationships that are embodied in the two Al-content (t) scales included in Figures 4 and 5.

TABLE 2. LINEAR REGRESSION EQUATIONS* FOR DETERMINATIVE CURVES

Monoclinic: Figure 4					Triclinic: Figure 5				
y**	x	m	c	R***	y	x	m	c	R
$\overline{T_1\text{–O}}$	b	-0.26564	5.1093	-0.965	$\overline{T_1\text{–O}}$	Y	-0.03233	4.5692	-0.986
t_1^J		-171.75	2266.3	-	t_1o^J		-20.852	1912.6	-
t_1^S		-195.75	2579.3	-	t_1o^S		23.764	2176.0	-
$\overline{T_2\text{–O}}$		0.28663	-2.0964	0.968	$\overline{T_1m\text{–O}}$		0.01905	-0.05438	0.982
t_2^J		184.68	-2384.2	-	t_1m^J		12.311	-1071.6	-
t_2^S		210.53	-2721.6	-	t_1m^S		14.028	-1224.7	-
$\overline{T_1\text{–O}}$	c	0.62037	-2.8055	0.974	$\overline{T_2\text{–O}}$		0.004266	1.2398	0.798
t_1^J		400.00	-2843.2	-	t_2^J		2.7356	-233.49	-
t_1^S		456.00	-3244.9	-	t_2^S		3.1180	-269.81	-
$\overline{T_2\text{–O}}$		-0.65590	6.3468	-0.957	$\overline{T_1\text{–O}}$	Y*	0.034383	-1.4349	-
t_2^J		-422.68	3056.4	-	t_1o^J		22.183	-1960.6	-
t_2^S		-481.73	3479.7	-	t_1o^S		25.281	-2238.1	-
$\overline{T_1\text{–O}}$	c*/b*	-1.0586	3.7851	-0.985	$\overline{T_1m\text{–O}}$		-0.020298	3.4872	-
t_1^J		-680.50	1402.2	-	t_1m^J		-13.097	1215.1	-
t_1^S		-776.00	1595.2	-	t_1m^S		-14.923	1380.9	-
$\overline{T_2\text{–O}}$		1.1305	-0.64384	0.977	$\overline{T_2\text{–O}}$		-0.0045106	2.0297	-
t_2^J		728.90	-1449.3	-	t_2^J		-2.9102	274.63	-
t_2^S		830.70	-1655.4	-	t_2^S		-3.3170	309.34	-
					$\overline{T_1\text{–O}}$	Δ	0.08080	1.6596	-
					t_1o^J		52.130	35.870	-
					t_1o^S		59.410	37.210	-
					$\overline{T_1m\text{–O}}$		-0.04770	1.6604	-
					t_1m^J		-30.777	36.390	-
					t_1m^S		-35.069	37.790	-
					$\overline{T_2\text{–O}}$		-0.01060	1.6237	-
					t_2^J		-6.8390	12.71	-
					t_2^S		-7.7950	10.81	-

*Equations are of the standard form y=mx+c.
**t_1^J and t_1^S are the Al-contents (wt.%) of site T_1 forecast from the 'modified Jones-Ribbe-Gibbs' (Al=645.16 $\overline{T\text{–O}}$ - 1034.84) and 'modified Smith-Bailey' (Al=735.29 $\overline{T\text{–O}}$ - 1183.09) curves respectively.
***correlation coefficients are not given for y=t_j and x=Y* and Δ because experimental standard deviations cannot be assigned to these parameters.

The determinative diagram for monoclinic K-feldspars (sanidines, orthoclases)

The tetrahedral Al-content t_j determinative diagram for the monoclinic K-feldspars (sanidines and orthoclases, including adularias) is constructed from data given in Table 1 according to the principles described above (Fig. 4). This diagram consists of plots against the unit-cell parameters b and c (Å) and the ratio c^*/b^* of the mean tetrahedral cation–oxygen distances $\overline{T_1\text{–O}}$ and $\overline{T_2\text{–O}}$ (Å) for the ten monoclinic K-feldspars whose structures have been refined. There are two t scales in addition to the $\overline{T\text{–O}}$ scale along the ordinate, one assuming the J–R–G and the other the S–B t versus $\overline{T\text{–O}}$ relationship as described in the preceding section. The reason $b/c \sin\beta$ and $6d_{060}/2d_{002}$ are included as equivalent to c^*/b^* is given below, where the use of the diagram is described. Linear regression lines are drawn through each group of corresponding plotted points, and

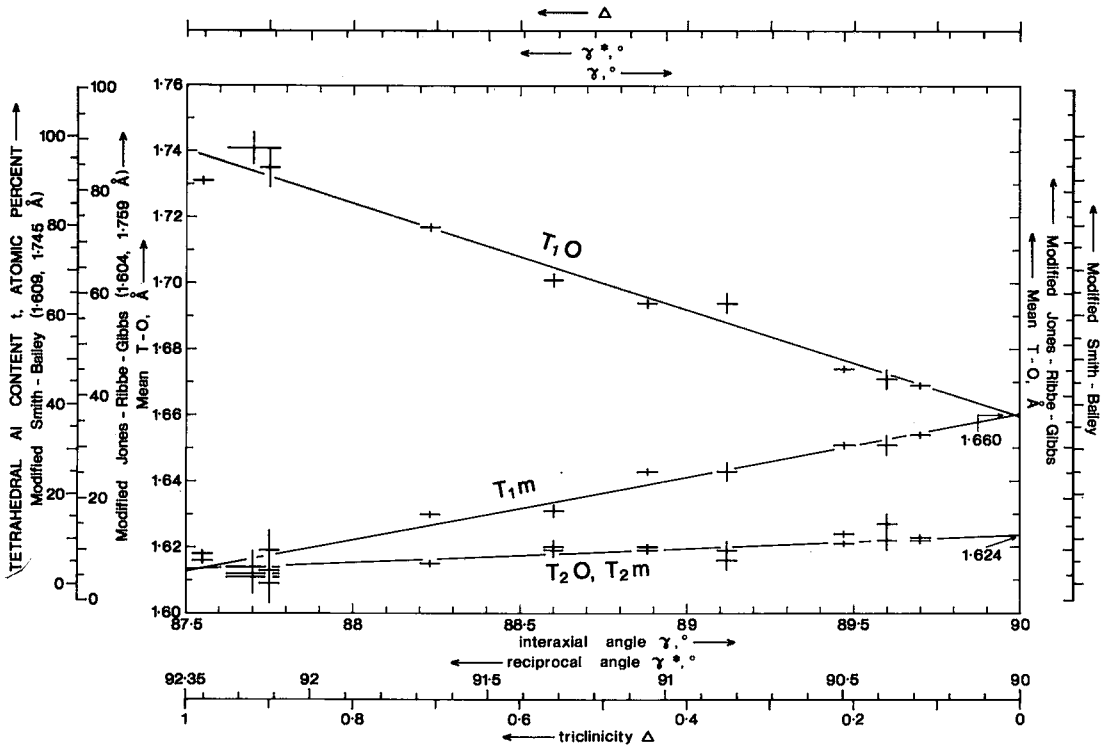

FIG. 5. Determinative diagram for microclines: plots with linear regression lines of the observed mean tetrahedral distance $\overline{T_1O\text{–}O}$, $\overline{T_1m\text{–}O}$, $\overline{T_2O\text{–}O}$ and $\overline{T_2m\text{–}O}$ (Å) against interaxial angle $\gamma(°)$ for the 10 structurally and geometrically triclinic K-feldspars whose structures have been refined. Data from Table 1. Bar lengths indicate standard deviations or errors. Only one regression line is included for the T_2O and T_2m points combined because of the closeness of corresponding $\overline{T_2O\text{–}O}$ and $\overline{T_2m\text{–}O}$ distances. As described in the text, additional ordinate scales are provided to read tetrahedral Al contents t_i (atomic %) assuming both the "modified Jones–Ribbe–Gibbs" (J–R–G) and the "modified Smith–Bailey" (S–B) t *versus* $\overline{T\text{–}O}$ relationships, and additional abscissa scales for γ^* and Δ are included for determinative purposes. Equations for the regression lines are given in Table 2. The diagram is discussed in the text.

equations for these lines are given in Table 2. The significance of some aspects of the regression lines is considered below under Discussion and Conclusions.

The determinative diagram for triclinic K-feldspars (microclines)

The tetrahedral Al-content t_i determinative diagram for the triclinic K-feldspars (microclines), constructed in the same manner as Figure 4, is shown as Figure 5. It consists of plots against the cell angle γ (°) (and two other abscissa scales explained below) of the mean tetrahedral cation–oxygen distances $\overline{T_1O\text{–}O}$, $\overline{T_1m\text{–}O}$, $\overline{T_2O\text{–}O}$ and $\overline{T_2m\text{–}O}$ (Å) for the 10 structurally and geometrically triclinic microclines whose structures have been refined. Again there are two t scales in addition to the T–O scale along the ordinate, one assuming the J–R–G and the other the S–B t *versus* $\overline{T\text{–}O}$ relationship. Linear regression lines are, as in Figure 4, drawn through each group of plotted points except that, because of the closeness of all $\overline{T_2O\text{–}O}$ and $\overline{T_2m\text{–}O}$ values to each other (Table 1), only one common regression line has been calculated and drawn for all T_2O and T_2m points. Equations are given in Table 2 for all the regression lines.

The left-hand limit of the diagram has been arbitrarily set at $\gamma = 87.5°$, which is slightly less (more extreme) than two of the smallest values recorded in the literature for maximum microclines, 87.60° [specimen Amaz A of Bachinski & Müller (1971) in Smith (1974), p. 233)], and 87.55° [specimen CA1E of Dal

Negro *et al.* 1978 (#21 in Table 1)]. This limiting value of $\gamma = 87.5°$ on the diagram is relevant to the other two scales that have been added to the abscissa for convenient determinative purposes, as described below. For the one additional scale, γ^*, it was necessary to choose a value for this reciprocal angle that could be regarded as corresponding to the chosen extreme γ angle of 87.5°. Extrapolation of the best straight line through a plot of γ^* (°) against γ (°) for 15 microclines, including the 10 geometrically triclinic ones in Table 1, suggested that $\gamma^* = 92.35°$ could reasonably be taken as corresponding to $\gamma = 87.5°$. This value of γ^* was thus used in constructing the γ^* abscissa scale in Figure 5, *which assumes a linear relationship between* γ^* *and* γ. For the other abscissa scale, that for the triclinicity $\Delta = 12.5(d_{131}-d_{1\bar{3}1})$ (a function of Å but usually taken as unitless: Goldsmith & Laves 1954), the extreme value of unity has again been arbitrarily equated with the chosen extreme value of γ, 87.5°, *also assuming a linear relationship.*

The use of the diagram is described in a succeeding section, and the significance of some aspects of the regression lines is considered below under Discussion and Conclusions.

Use of the determinative diagrams

In general, the diagrams shown in Figures 4 and 5 and the corresponding equations given in Table 2 are intended to provide a rapid means of determining the individual tetrahedral Al contents t_1 and t_2 in monoclinic K-feldspars (sanidines, orthoclases, adularias), and t_1O, t_1m and $t_2O = t_2m$ in triclinic K-feldspars (microclines), all with Or $\geqslant \sim$ 85 mole %, from precise unit-cell parameters obtained by any standard means but most commonly by the computer refinement of X-ray powder data. Such determinative methods can be used to characterize structurally in a rapid way large numbers of K-feldspars in a given suite of, for example, granitic and gneissic rocks.

Although the curves reproduced in Figures 4 and 5 may be used to derive $\overline{T_j\text{–O}}$ and t_j values graphically for a particular K-feldspar from the appropriate cell parameter(s), the obvious procedure is to use the relevant linear regression equations(s) in Table 2 to calculate the derived values. Applying the method, the user may derive $\overline{T_j\text{–O}}$ values first, or he can derive t_j values directly, using either the J–R–G or the S–B *t versus* $\overline{T\text{–O}}$ relationship. For reasons given below, the author *much prefers* the J–R–G to the S–B *t versus* $\overline{T\text{–O}}$ relationship.

For monoclinic K-feldspars (sanidines, orthoclases, adularias), Figure 4 and Table 2 indicate that it is possible to use either or both cell periods b or c (Å) to derive, for a particular monoclinic K-feldspar, $\overline{T_1\text{–O}}$, $\overline{T_2\text{–O}}$ and t_1, t_2. Cell period b is the more sensitive and should give the more precise result. However, because b and c vary in opposite senses with increase in t_1 and decrease in t_2, *i.e.*, with increasing Si/Al ordering, a more sensitive parameter than either b or c alone is one with b and c in reciprocal relationship. The writer has followed the usage of Jones (1966) in utilizing the reciprocal parameter ratio c^*/b^*. This ratio can easily be used in this form from the output of standard computer programs for the refinement of powder data. However, this ratio of reciprocal parameters may be expressed in terms of direct lattice spacings: $c^*/b^* = b/c\sin\beta = d_{010}/d_{001} = 6d_{060}/2d_{002}$. If it is recognized that 060 and 002 are prominent resolved reflections in the powder patterns of sanidines and some orthoclases or adularias (see, for example, Borg & Smith 1969), then one can readily calculate the ratio $6d_{060}/2d_{002} = c^*/b^*$ from the spacings of these lines alone without refining a large amount of the powder data. Furthermore, because this parameter utilizes a *ratio* of two lattice spacings rather than an absolute value of a single cell parameter such as b or c, it is less sensitive to instrumental error, and the use of an internal standard is not as important as in the case of a single parameter. However, for any monoclinic K-feldspars where reflection 002 is not clearly resolved on the powder pattern, the user is strongly advised either to derive c^*/b^* by computer refinement of all the available powder data or to use the following shorter procedure.

This procedure involves the use of the prominent powder reflection 060 that occurs on the patterns of all K-feldspars at 2θ(Cu $K\alpha$) $\sim 41\frac{1}{2}°$ and that is either well resolved or partly overlapped only by reflection 003, which is of negligible intensity. A value of d_{060} (Å) derived from a powder pattern obtained with an internal standard or similar device can be used to give $b = 6d_{060}$ (Å) which can be applied to the b curve in Figure 4 to yield $\overline{T_1\text{–O}}$, $\overline{T_2\text{–O}}$ and t_1, t_2. In the use of the single reflection 060 (with, say, an internal standard reflection) to derive t_1 and t_2, the operator should record the whole powder pattern and not just the small angular range that includes 060 and the standard reflection, in order to

ensure that the specimen is truly a monoclinic K-feldspar.

For triclinic K-feldspars (microclines), Figure 5 and Table 2 can be used to derive, for a particular microcline, values of $\overline{T_1O\text{–}O}$, $\overline{T_1m\text{–}O}$ and $\overline{T_2O\text{–}O} = \overline{T_2m\text{–}O}$ and corresponding t_1O, t_1m and $t_2O = t_2m$ from the (direct) interaxial angle γ, obtained most commonly from computer-refined powder data. This is the recommended procedure because, in the preparation of Figure 5, the experimental $\overline{T_j\text{–}O}$ values were plotted against γ, not against the other two abscissa units γ^* and Δ. However, as explained above, because reciprocal interaxial angle γ^* and triclinicity $\Delta = 12.5(d_{131}-d_{1\bar{3}1})$ are commonly used in addition to γ to characterize microclines, scales for these two parameters are also included in Figure 5 and Table 2. Strictly speaking, $\overline{T_j\text{–}O}$ and t_j values derived from using the γ^* and Δ scales will not be as precise as those derived from the γ scale (because of the manner of relating the former to the latter), but in practice the derived values should be nearly as precise, provided a conservative estimate of the accuracy is used for γ; this is considered further below.

Just as it is possible to derive $\overline{T_j\text{–}O}$ and t_j values of a monoclinic K-feldspar without refining the powder data (by using d_{060} and d_{002}), so it is possible to derive these values directly for a microcline by using the triclinicity Δ. The reason is the same as in the monoclinic case, namely, that the parameter Δ can be obtained readily from two prominent reflections on the X-ray powder pattern, 131 and $1\bar{3}1$ (Borg & Smith 1969); again, an internal standard is not as necessary as when a single absolute unit-cell parameter is used because Δ is a function of the difference between two spacings (d_{131} and $d_{1\bar{3}1}$). However, the use of an internal standard or similar device is again recommended to enhance the accuracy of the results. Also, as in the case of a monoclinic K-feldspar, if there is any question about the resolution of the reflections in question, which is likely to be the situation where $\Delta < \sim 0.2$, the user should computer-process all the available powder data, and then use the parameter γ.

TABLE 3. PROBABLE ERRORS IN DERIVED TETRAHEDRAL DISTANCES $\overline{T_j\text{–}O}$ (Å) AND Al-CONTENTS t_j (%)

K FELDSPAR	(1)	(2)	(3)	(4)	(5a)	(5b)
MONOCLINIC SANIDINES/ ORTHOCLASES	b, (Å) computer refined	0.007Å	T_1, T_2	0.001_9	1.2	1.4
	$6d_{060}$ from powder pattern	0.01Å	T_1, T_2	0.002_7	1.7	2.0
	c, Å computer refined	0.004Å	T_1, T_2	0.002_5	1.6	1.8
	c*/b* from computer refined data	0.001_5Å	T_1, T_2	0.001_6	1.0	1.2
TRICLINIC MICROCLINES	γ computer refined	0.07°	T_1O	0.002_3	1.5	1.7
			T_1m	0.001_3	0.8	1.0
			T_2O, T_2m	0.000_3	0.2	0.2

CONCLUDED REASONABLE PROBABLE ERRORS:

$\Delta(\overline{T_j\text{–}O}) = 0.003$Å

Δt_j = 3 Al atoms of % Al deduced (for a particular $t/\overline{T\text{–}O}$ relationship)

(1) determinative cell parameter; (2) usual σ or "standard error" (powder data); (3) T_j site(s); (4) derived difference $\Delta(\overline{T_j\text{–}O})$, Å (Figs. 4,5, Table 2); (5) corresponding derived difference Δt_j (%) assuming $t/\overline{T\text{–}O}$ of J-R-G (5a) and of S-B (5b).

Probable errors in tetrahedral distances $\overline{T_j\text{–}O}$ and Al contents t_j derived from the diagrams

In Table 1 the numbers in brackets following the values of unit-cell parameters and mean interatomic distances are variously described by the original authors as "standard deviations σ", or "standard errors" or "estimated standard errors". If one assumes these terms to be more or less equivalent, then from Table 1 it is possible to choose, for a given unit-cell parameter such as b, some general value of the "error" that can be used as a basis for determining the probable error in derived distances $\overline{T_j\text{–}O}$ and Al contents t_j. However, since determinative diagrams such as those described here are intended for use with unit-cell parameters derived from computer-refined X-ray powder data, the likely error in the parameters is better taken from sets of parameters derived in this way, such as those given in Table II of Stewart & Wright (1974) or in Table II of Cherry & Trembath (1978). Likely errors in the relevant unit-cell parameters deduced from these sources are given in Table 3 under the column "usual σ" or "standard error". When applied to the determinative diagrams (Figs. 4, 5), these likely errors in unit-cell parameters yield values of the "derived difference $\Delta(\overline{T_j\text{–}O})$, Å", and the corresponding "derived difference in Al content Δt_j, %" given in Table 3. From these values and from the presumed error in the curves in Figures 4 and 5, one may conclude that the application of computer-refined X-ray powder data to these determinative curves should yield, *in general*, mean tetrahedral-oxygen distances $\overline{T_j\text{–}O}$ within about 0.003 Å, and individual tetrahedral Al contents t_j (in %) within about 3 Al atoms of the t_j value deduced for a given t *versus* $\overline{T\text{–}O}$ relationship (J–R–G *or* S–B). As

discussed below, the least reliable results are likely to pertain to K-feldspars that are structurally triclinic but geometrically monoclinic ($\alpha=\gamma=90°$). Greater errors and even misleading $\overline{T_j\text{–O}}$ and t_j values could be obtained by applying determinative curves of this type to such unusual structures.

Discussion and Conclusions

The complication of structurally triclinic ($\overline{T_1O\text{–}O} \neq \overline{T_1m\text{–}O}$), geometrically monoclinic ($\alpha=\gamma=90°$) K-feldspars

Three of the nine K-feldspars whose structures were refined by Dal Negro *et al.* (1978) (see Table 1 for the relevant data) are of the type described by the above subheading. Any tetrahedral Al-content determinative method that utilizes unit-cell parameters must yield erroneous Al contents, because the geometry will imply two structurally equivalent monoclinic sites T_1, whereas the structure will in fact have two nonequivalent triclinic sites T_1O and T_1m.

It is instructive to look at the three K-feldspars of this type described by Dal Negro *et al.* (1978) by applying the relevant data for them given in Table 1 to the new determinative curves (Figs. 4, 5). There are two ways of doing this. The first is to treat the geometry at face value, *i.e.*, as monoclinic, and use the curves in Figure 4 to extract $\overline{T_j\text{–O}}$ and t_j (monoclinic) from c^*/b^* parameters and then compare these with the observed values (triclinic) in Table 1. The results are shown in Table 4, where it may be seen that the derived $\overline{T_1\text{–O}}$ distances differ by as much as 0.008 Å from the observed $\overline{T_1O\text{–O}}$ and $\overline{T_1m\text{–O}}$ distances, although most differences are $\leqslant 0.005$ Å. The differences between the derived $\overline{T_2\text{–O}}$ and observed $\overline{T_2O\text{–O}}$ and $\overline{T_2m\text{–O}}$ distances are only $\leqslant 0.002$ Å. The differences in derived and observed Al contents t_j reflect, of course, the T_j–O differences: derived t_1 values differ from observed t_1O and t_1m by as much as 5 atom % but more usually by 3 atom % or less, and derived t_2 differs from observed t_2O and t_2m by 1 atom % or less.

The other way of applying the data for these three structurally triclinic, geometrically monoclinic K-feldspars to the new determinative curves is to fit the triclinic T_j–O values observed by Dal Negro *et al.* (1978) to the curves for the triclinic cases in Figure 5 and to extract the corresponding angle γ in order to see how much it departs from 90° (*i.e.*, monoclinic). When the observed mean tetrahedral distances $\overline{T_1O\text{–O}}$, $\overline{T_1m\text{–O}}$ and $\overline{T_2'\text{–O}}$ for the three specimens P2B, P2A and CA1A (Table 1) are fitted mathematically to the three curves in Figure 5, the best fits are found to occur at 89.97, 89.81 and 89.70°, respectively. Dal Negro *et al.* estimated their experimental error in γ^* (which can also be taken for γ) as $\sim 2' = 0.03°$, and since the departures of the angles for the $\overline{T_j\text{–O}}$ values fitted to the curves in Figures 5 are 0.03, 0.19 and 0.30° for the three specimens, respectively, it can be seen that, for some inexplicable reason, the geometries of at least two of these specimens, P2A and CA1A, do not reflect their structurally triclinic character.

Dal Negro *et al.* (1978) do not comment on whether optical or any other characteristics of these three K-feldspars provide a clue to their true triclinic nature. De Pieri & Callegari (1977), in an optical and X-ray-diffraction investigation of these and many other K-feldspars from the same Adamello massif, observed that specimen P2 (from which Dal Negro's crystals P2A and P2B were obtained for structure analysis) is optically monoclinic with triclinicity $\Delta = 0$, whereas specimen CA1 (the source of CA1A) is "Or/Micr." optically and has Δ in the range 0–0.63. It appears from this that one cannot suspect from optical or other evidence that a "geometrically monoclinic" K-feldspar is in fact structurally triclinic.

From these observations about these three K-feldspars, one may conclude that some (presumably only a few) K-feldspars that give monoclinic orthoclase-like powder patterns will in fact be triclinic. For such specimens, the errors in $\overline{T_1O\text{–O}}$, $\overline{T_1m\text{–O}}$ and t_1O, t_1m values

TABLE 4. APPLICATION TO THE DETERMINATIVE CURVES OF THE DATA FOR THE THREE STRUCTURALLY TRICLINIC, GEOMETRICALLY MONOCLINIC K FELDSPARS OF DAL NEGRO ET AL. (1978)

(1)	(2)	(3)	(4a) (4b)	(5)	(6a) (6b)	(7)	(8a) (8b)	(9)	(10a) (10b)
P2B	2.0121	1.655	1.660 1.657	1.631	1.631 1.630	33	36 34	17	17 17
P2A	2.0073	1.660	1.665 1.655	1.625	1.626 1.626	36	39 33	14	14 14
CAIA	2.0033	1.664	1.672 1.659	1.621	1.623 1.623	39	44 35	11	12 12

(1) specimen; (2) c^*/b^* (=b/csinβ); (3) derived $\overline{T_1\text{–O}}$ (Å); (4a), (4b) observed $\overline{T_1O\text{–O}}$, $\overline{T_1m\text{–O}}$ (Å)(Dal Negro); (5) derived $\overline{T_2\text{–O}}$(Å); (6a), (6b) observed $\overline{T_2O\text{–O}}$, $\overline{T_2m\text{–O}}$ (Å) (Dal Negro); (7) derived t_1 (%)*; (8a), (8b) deduced t_1O, t_1m (%) (Dal Negro)+; (9) derived t_2 (%)*; (10a), (10b) deduced t_2O, t_2m (%) (Dal Negro)+.

*assuming the J-R-G $t/\overline{T\text{–O}}$ relationship

+the t_j (%) values given here differ slightly from those of Dal Negro et al. (1978, Table 9) because the former assume the J-R-G $t/\overline{T\text{–O}}$ relationship and the latter in effect the S-B relationship.

derived from the application of their cell parameters to the curves in Figures 4 and 5 will be appreciably greater than the likely errors given in the preceding section (*i.e.*, 0.003 Å and 3 Al atom%); they may attain 0.008 Å and 5 Al atom %.

The likely b and c periods of completely disordered (high) sanidine

Each of the pair of *b* and *c* tetrahedral cation–oxygen distance curves $\overline{T_1\text{–O}}$ and $\overline{T_2\text{–O}}$ (Å) for the monoclinic K-feldspars in Figure 4 converge at a $\overline{T_j\text{–O}}$ value of 1.643_3 Å, which is, as one would expect, the same as the grand mean $\overline{T_j\text{–O}}$ distance for all tetrahedra for all 23 K-feldspars included in Table 1. The convergence points for the pairs of $\overline{T_1\text{–O}}$ and $\overline{T_2\text{–O}}$ lines for each of *b* and *c* in Figure 4 correspond to a completely Si/Al disordered monoclinic K-feldspar, that is, to a sanidine, or what is sometimes termed a high sanidine (see Smith 1974, chapter 9). One might then expect the *b* and *c* lattice periods corresponding to these convergence points to be those of a completely disordered (high) sanidine; these are: $b = 13.047$, $c = 7.171$ Å. It is difficult to estimate a likely variation in these values, but one might conclude from Table 1 and Figure 4 that, for a sanidine with Or $\geqslant \sim 85$ mole % and with only minor amounts of Ca, Ba, *etc.*, these values are likely to hold within ~ 0.003 Å. These two theoretical cell dimensions are more extreme, larger for *b* and smaller for *c*, than some of the most extreme values reported in the literature for (high) sanidines, all synthetic (see Smith 1974, Table 7–2):

	b(Å)	c(Å)
Kroll (1973) observed	13.031(1)	7.175(1)
extrapolated	13.033	7.174
Henderson (1979)	13.026(1)	7.178(1)

A comparison of these extreme observed *b* and *c* periods with the theoretical values derived from Figure 4 suggests that even these synthetic specimens are not completely Si/Al disordered.

Orthoclase as the monoclinic end-member of the triclinic microcline series

The $\overline{T_1\text{O–O}}$ and $\overline{T_1m\text{–O}}$ mean distance curves for microclines in Figure 5 converge at $\gamma = 90°$ at values of 1.6596 Å and 1.6604 Å, respectively; that is, both curves can be taken as converging at $\gamma = 90°$ at a $\overline{T_j\text{–O}}$ distance of 1.660 Å. The single curve for $\overline{T_2'\text{–O}}$ ($\overline{T_2\text{O–O}}$ and $\overline{T_2m\text{–O}}$ combined) intersects the ordinate at $\gamma = 90°$ at a value of 1.6237 Å, *i.e.*, 1.624 Å. These convergence and intersecting $\overline{T_j\text{–O}}$ values at $\gamma = 90°$ indicate that the theoretical end-member of the maximum microcline – intermediate microcline triclinic structural series can be taken as a structure with two pairs of equivalent *T* sites, T_1 and T_2; that is, it would be monoclinic, with $\overline{T_1\text{–O}} = 1.660$, $\overline{T_2\text{–O}} = 1.624$ Å. One might then ask, do these monoclinic $\overline{T_j\text{–O}}$ distances correspond to any actual refined structures? Table 1 and Figure 4 (plotted circles) show that the $\overline{T_1\text{–O}}$ and $\overline{T_2\text{–O}}$ distances in two of the refined monoclinic K-feldspars are within 2σ of these theoretical values: orthoclase, Spencer C (sample 7) and adularia, Spencer B (sample 8) have respective $\overline{T_1\text{–O}}$ and $\overline{T_2\text{–O}}$ values of 1.656(3), 1.628(3) Å and 1.664(2), 1.622(2) Å. The first six monoclinic structures in Table 1 have $\overline{T_1\text{–O}}$ and $\overline{T_2\text{–O}}$ values that fall between the above theoretical values, 1.660, 1.624 Å and the $\overline{T_j\text{–O}}$ for both tetrahedra in disordered (high) sanidine, 1.643 Å (see preceding section), and so they may be considered as intermediate in Si/Al order between the fully disordered end-member and the feldspar whose degree of order corresponds to the two theoretical $\overline{T_j\text{–O}}$ distances, 1.660, 1.624 Å (discussed below). The two $\overline{T_j\text{–O}}$ distances in the remaining two (structurally) monoclinic K-feldspars in Table 1, adularia 7007 (sample 9) and ordered orthoclase (sample 10), have $\overline{T_1\text{–O}}$ and $\overline{T_2\text{–O}}$ values somewhat larger and smaller, respectively, 1.665(1), 1.621(1) Å and 1.667(1), 1.616(1) Å, than the theoretical values. However, despite the poor agreement of the theoretical $\overline{T_j\text{–O}}$ distances with those for these two K-feldspars, the good agreement of the theoretical with the observed values for samples 7 and 8 in combination with the nature of the curves in Figure 5 lead the author to conclude that the *structural end-member of the triclinic microcline series can reasonably be interpreted as monoclinic orthoclase*. This matter is discussed further in relation to Si/Al ordering in the section that follows.

An interpretation in terms of Si/Al ordering

Orthoclase: Table 1 shows the Al contents t_1 and t_2 (atomic %) in the analyzed monoclinic K-feldspar structures according to what are, in effect, the two different *t versus* $\overline{T\text{–O}}$ relationships in general use. The two orthoclase/adularia structures (samples 7 and 8) whose $\overline{T_j\text{–O}}$ values are closest to the theoretical ones derived from Figure 5 have $t_1 = 37 \pm 3$ and t_2

$= 13 \pm 3\%$ Al, the variation taking account of the t_j values for both assumed *t versus* $\overline{T\text{–O}}$ relationships. The theoretical $\overline{T_j\text{–O}}$ values of 1.660, 1.624 Å from Figure 5 yield t_1 and t_2 values of 36, 13 and 37½, 11% Al atoms, assuming the J–R–G and the S–B *t versus* $\overline{T\text{–O}}$ relationships, respectively. These figures suggest that the K-feldspar here called orthoclase has $t_1 \sim 37$ and $t_2 \sim 13\%$ Al. In close agreement with these Al contents are those predicted over twenty years ago from theoretical bond-strength considerations by Ferguson *et al.* (1958) for "ideal orthoclase", namely, $t_1 = 36$ and $t_2 = 14\%$ Al. The author therefore concludes that the refinement of certain orthoclase and adularia structures, the theoretical $\overline{T_j\text{–O}}$ values for the monoclinic end-member of the triclinic microcline series and the earlier proposed bond-strength model of K-feldspars all point strongly to *the existence of orthoclase as a monoclinic structure that is partly Si/Al ordered with* $t_1 \sim 36$ *and* $t_2 \sim 14\%$ *Al.* The evidence presented here mitigates against the existence of a fully ordered monoclinic orthoclase, that is, one with $t_1 = 50$ and $t_2 = 0\%$ Al, which has been the subject of much discussion and controversy (see, for example, Prince *et al.* 1973, Martin 1974, Smith 1974, chapter 9).

Microcline: Maximum microcline is the most fully Si/Al ordered of the K-feldspars. It may be seen from Table 1 that the most ordered of the microclines whose structures have been refined, sample 23, has t_1O equal to only 88% Al, assuming the J–R–G *t versus* $\overline{T\text{–O}}$ relationship, although it equals 98% Al assuming the S–B relationship. The difference between these two values emphasizes the large differences in t_j values that can result from a given $\overline{T_j\text{–O}}$ value for more-or-less fully ordered K-feldspars from the use of different *t versus* $\overline{T\text{–O}}$ relationships. In the preceding section it was pointed out that the theoretical Al contents t_1 and t_2 predicted two decades ago for monoclinic orthoclase using a bond-strength interpretation of the structures agree closely with those for refined orthoclase structures and for a theoretical monoclinic end-member of the triclinic microcline series. The author regards this agreement as supporting evidence for the validity of the bond-strength interpretation of the K-rich (and Na-rich) feldspar structures. The application of the bond-strength theory to the microcline structure by the author in the same paper (Ferguson *et al.* 1958) and in others (Ferguson 1960; see also Gait *et al.* 1970) suggests that the most ordered maximum microcline is not, as is widely assumed, fully Si/Al ordered with t_1O $\sim$ 100% Al but rather only *largely* ordered with t_1O only 75–82% Al, *i.e.*, $\sim$ 80% Al. Because this figure of $\sim$ 80% Al for t_1O can be taken as only approximate considering the assumptions involved, and because the three most ordered maximum microclines in Table 1 (the last three entries) have, assuming the widely used (in effect) J–R–G *t versus* $\overline{T\text{–O}}$ relationship, t_1O values of 88, 85 and 82% Al, the author concludes that *maximum microcline can reasonably be interpreted, as not fully, but only largely, Si/Al ordered, with* t_1*O in the range 80–85% Al.* Furthermore, because the structure refinements of the K-feldspars and the nature of the determinative curves in Figures 4 and 5 conform, in the author's opinion, to the earlier proposed bond-strength interpretation of the alkali feldspars, and because the J–R–G *t versus* $\overline{T\text{–O}}$ relationship gives t_j values closer to those expected from this bond-strength interpretation than does the S–B, *the author strongly prefers the modified Jones–Ribbe–Gibbs (J–R–G) to the modified Smith–Bailey (S–B) t versus* $\overline{T\text{–O}}$ *relationship (Figs. 4, 5,* Table 2).

Possible genetic implications of derived tetrahedral Al contents t_j

The t_j determinative method described here (Figs. 4, 5, Table 2) enables one to derive rapidly the tetrahedral Al contents t_1 and t_2 in monoclinic K-rich feldspars (sanidines, orthoclases, adularias) or t_1O, t_1m, t_2O $= t_2m$ in triclinic K-rich feldspars (microclines), which structurally characterize that K-feldspar in a specific way. In the light of t_j values determined for a particular K-feldspar specimen, or more usually for a suite of such specimens, from one granitic batholith, for example, the observer may make a genetic interpretation of the results according to some model, including that of Stewart & Wright (1974), as those authors and several others have done, *e.g.*, Cherry & Trembath (1978, 1979) and Mehta (1979). However, the author disagrees with this widely accepted model and prefers a fundamentally different one based on a bond-strength interpretation of the alkali feldspar structures, as discussed in the preceding section. Rather than interpreting the derived Si/Al distributions (Al contents t_j) of a single specimen or a suite of K-feldspar(s) in terms of the series Si/Al-disordered sanidine → (fully) ordered maximum microcline in terms of high-to-low temperatures in the manner of Stewart & Wright (1974) and most others, the bond-strength theory leads to

an interpretation of the Si/Al distributions in terms of a series Si/Al-disordered sanidine → partly ordered orthoclase from high to low temperatures in a K-rich environment. The theory also interprets the distributions in terms of a series partly ordered orthoclase → largely ordered maximum microcline at low temperatures in environments varying from K-rich, Na-poor to Na-rich, K-poor. Because these ideas have been published elsewhere, the author leaves it to the interested reader to consult the papers that describe the bond-strength model of the alkali feldspars (Ferguson *et al.* 1958; Ferguson 1960, 1979).

Acknowledgements

The author is indebted to Dr. J.B. Jones for making possible his year at the University of Adelaide, and for invaluable discussions on the feldspars. He is also indebted to Miss A.M.C. Swan, Mr. R. Barrett and Miss M. Stanley in Adelaide for technical assistance, and to Dr. F.C. Hawthorne and to Mrs. S. Fay, Mrs. M. Gray and Mrs. V. Truelove in Winnipeg for valued professional consultation and technical assistance, respectively. The author expresses his appreciation to L.J. Cabri, acting editor D.C. Harris, associate editors B.J. Wuensch and F.C. Hawthorne, and two referees for suggestions and assistance that greatly improved the final form of the paper. Finally, he also thanks the British Council for a Commonwealth University Interchange Travel Grant, and the Natural Sciences and Engineering Research Council of Canada for continuing financial support.

References

Bachinski, S.W. & Müller, G. (1971): Experimental determinations of the microcline – low albite solvus. *J. Petrology* **12**, 329-356.

Bailey, S.W. (1969): Refinement of an intermediate microcline structure. *Amer. Mineral.* **54**, 1540-1545.

——— & Taylor, W.H. (1955): The structure of a triclinic potassium feldspar. *Acta Cryst.* **8**, 621-632.

Blasi, A. (1978): Structural explanation for $\Delta(\alpha^*\gamma^*)$ from α^* *vs.* γ^* in alkali feldspar. *Tschermaks Mineral. Petrog. Mitt.* **25**, 47-56.

——— & Blasi De Pol, C. (1977): Role and convenience of lattice elements for deriving Si, Al distribution in alkali feldspar. *Rend. Soc. Ital. Mineral. Petrologia* **33**, 497-509.

Borg, I.Y. & Smith, D.K. (1969): Calculated X-ray powder patterns for silicate minerals. *Geol. Soc. Amer. Mem.* **122**.

Brown, B.E. & Bailey, S.W. (1964): The structure of maximum microcline. *Acta Cryst.* **17**, 1391-1400.

Brown, G.E., Hamilton, W.C., Prewitt, C.T. & Sueno, S. (1974): Neutron diffraction study of Al/Si ordering in sanidine: a comparison with X-ray diffraction data. *In* The Feldspars (W.S. MacKenzie & J. Zussman, eds.), Manchester Univ. Press, Manchester, England.

Cherry, M.E. & Trembath, L.T. (1978): Structural state and composition of alkali feldspars in granites of the St. George pluton, southwestern New Brunswick. *Mineral. Mag.* **42**, 391-399.

——— & ——— (1979): Order–disorder paths of alkali feldspars. *Amer. Mineral.* **64**, 66-70.

Cole, W.F., Sörum, H. & Kennard, O. (1949): The crystal structures of orthoclase and sanidinized orthoclase. *Acta Cryst.* **2**, 280-287.

Colville, A.A. & Ribbe, P.H. (1968): The crystal structure of an adularia and a refinement of the structure of orthoclase. *Amer. Mineral.* **53**, 25-37.

Dal Negro, A., De Pieri, R., Quareni, S. & Taylor, W.H. (1978): The crystal structures of nine K feldspars from the Adamello massif (northern Italy). *Acta Cryst.* **B34**, 2699-2707.

De Pieri, R. & Callegari, E. (1977): Potassium feldspars from the igneous rocks of the Adamello massif (northern Italy). II. Optical and crystallographical observations. *Ist. Geol. Mineral. Univ. Padova, Mem.* **32**, 3-15.

Ferguson, R.B. (1960): The low-temperature phases of the alkali feldspars and their origin. *Can. Mineral.* **6**, 415-436.

——— (1979): Whence orthoclase and microcline? A crystallographer's interpretation of potassium feldspar phase relations. *Can. Mineral.* **17**, 515-525.

———, Traill, R.J. & Taylor, W.H. (1958): The crystal structures of low-temperature and high-temperature albites. *Acta Cryst.* **11**, 331-348.

Finney, J.J. & Bailey, S.W. (1964): Crystal structure of an authigenic maximum microcline. *Z. Krist.* **119**, 413-436.

Gait, R.I., Ferguson, R.B. & Coish, H. (1970): Electrostatic charge distributions in the structure of low albite. *Acta Cryst.* **B26**, 68-77.

GOLDSMITH, J.R. & LAVES, F. (1954): Potassium feldspars structurally intermediate between microcline and sanidine. *Geochim. Cosmochim. Acta* **6**, 100-118.

HENDERSON, C.M.B. (1979): An elevated temperature X-ray study of synthetic disordered Na–K alkali feldspars. *Contr. Mineral. Petrology* **70**, 71-79.

HOVIS, G.L. (1974): A solution calorimetric and X-ray investigation of Al–Si distribution in monoclinic potassium feldspars. *In* The Feldspars (W.S. MacKenzie & J. Zussman, eds.), Manchester Univ. Press, Manchester, England.

JONES, J.B. (1966): Order in alkali feldspars. *Nature* **210**, 1352-1353.

——— (1968): Al–O and Si–O tetrahedral distances in aluminosilicate framework structures. *Acta Cryst.* B**24**, 355-358.

——— & TAYLOR, W.H. (1961): The structure of orthoclase. *Acta Cryst.* **14**, 443-456.

KROLL, H. (1973): Estimation of the Al, Si distribution of feldspars from the lattice translations Tr[110] and Tr[1$\bar{1}$0]. I. Alkali feldspars. *Contr. Mineral. Petrology* **39**, 141-156.

———(1980): Estimation of the Al,Si distribution of alkali feldspars from lattice translations tr[110] and tr[1$\bar{1}$0]. Revised diagrams. *Neues Jahrb. Mineral. Monatsh.*, 31-36.

MARTIN, R.F. (1974): Controls of ordering and subsolidus phase relations in the alkali feldspars. *In* The Feldspars (W.S. MacKenzie & J. Zussman, eds.), Manchester University Press, Manchester, England.

MEHTA, P.K. (1979): X-ray and optical studies of feldspars from the gneissic rocks of Kulu, N.W. Himalaya, India. *Neues Jahrb. Mineral. Abh.* **135**, 88-112.

ORVILLE, P.M. (1967): Unit-cell parameters of the microcline–low albite and the sanidine–high albite solid solution series. *Amer. Mineral.* **52**, 55-86.

PHILLIPS, M.W. & RIBBE, P.H. (1973): The structures of monoclinic potassium-rich feldspars. *Amer. Mineral.* **58**, 263-270.

PRINCE, E., DONNAY, G. & MARTIN, R.F. (1973): Neutron diffraction refinement of an ordered orthoclase structure. *Amer. Mineral.* **58**, 500-507.

RIBBE, P.H. (1963): A refinement of the crystal structure of sanidinized orthoclase. *Acta Cryst.* **16**, 426-427.

——— (1975): The chemistry, structure and nomenclature of feldspars. *In* Feldspar Mineralogy (P.H. Ribbe, ed.), *Mineral. Soc. Amer. Short Course Notes* **2**, R1-52.

——— (1979): The structure of a strained intermediate microcline in cryptoperthitic association with twinned plagioclase. *Amer. Mineral.* **64**, 402-408.

——— & GIBBS, G.V. (1969): Statistical analysis and discussion of mean Al/Si–O bond distances and the aluminum content of tetrahedra in feldspars. *Amer. Mineral.* **54**, 85-94.

——— & ——— (1975): The crystal structure of a strained intermediate microcline in cryptoperthitic association with low albite. *Geol. Soc. Amer. Abstr. Programs* **7**, 1245.

———, PHILLIPS, M.W. & GIBBS, G.V. (1974): Tetrahedral bond length variations in feldspars. *In* The Feldspars (W.S. MacKenzie & J. Zussman, eds.). Manchester University Press, Manchester, England.

SMITH, J.V. (1974): *Feldspar Minerals. 1. Crystal Structure and Physical Properties.* Springer-Verlag, New York.

——— & BAILEY, S.W. (1963): Second review of Al–O and Si–O tetrahedral distances. *Acta Cryst.* **16**, 801-811.

STEWART, D.B. (1975): Lattice parameters, composition and Al/Si order in alkali feldspars. *In* Feldspar Mineralogy (P.H. Ribbe, ed.), *Mineral. Soc. Amer. Short Course Notes* **2**, St 1-22.

——— & RIBBE, P.H. (1969): Structural explanation for variations in cell parameters of alkali feldspar with Al/Si ordering. *Amer. J. Sci.* **267–A**, 444-462.

——— & WRIGHT, T.L. (1974): Al/Si order and symmetry of natural alkali feldspars, and the relationships of strained cell parameters to bulk composition. *Soc. franç. Minéral. Crist. Bull.* **97**, 356-377.

WEITZ, G. (1972): Die Struktur des Sanidins bei verschiedenen Ordnungsgraden. *Z. Krist.* **136**, 418-426.

WRIGHT, T.L. & STEWART, D.B. (1968): X-ray and optical study of alkali feldspar. I. Determination of composition and structural state from refined unit-cell parameters and 2V. *Amer. Mineral.* **53**, 38-87.

Received April 1980, revised manuscript accepted September 1980.

GLOSSARY: CRYSTALLOGRAPHIC NOTATION FOR THE K FELDSPARS

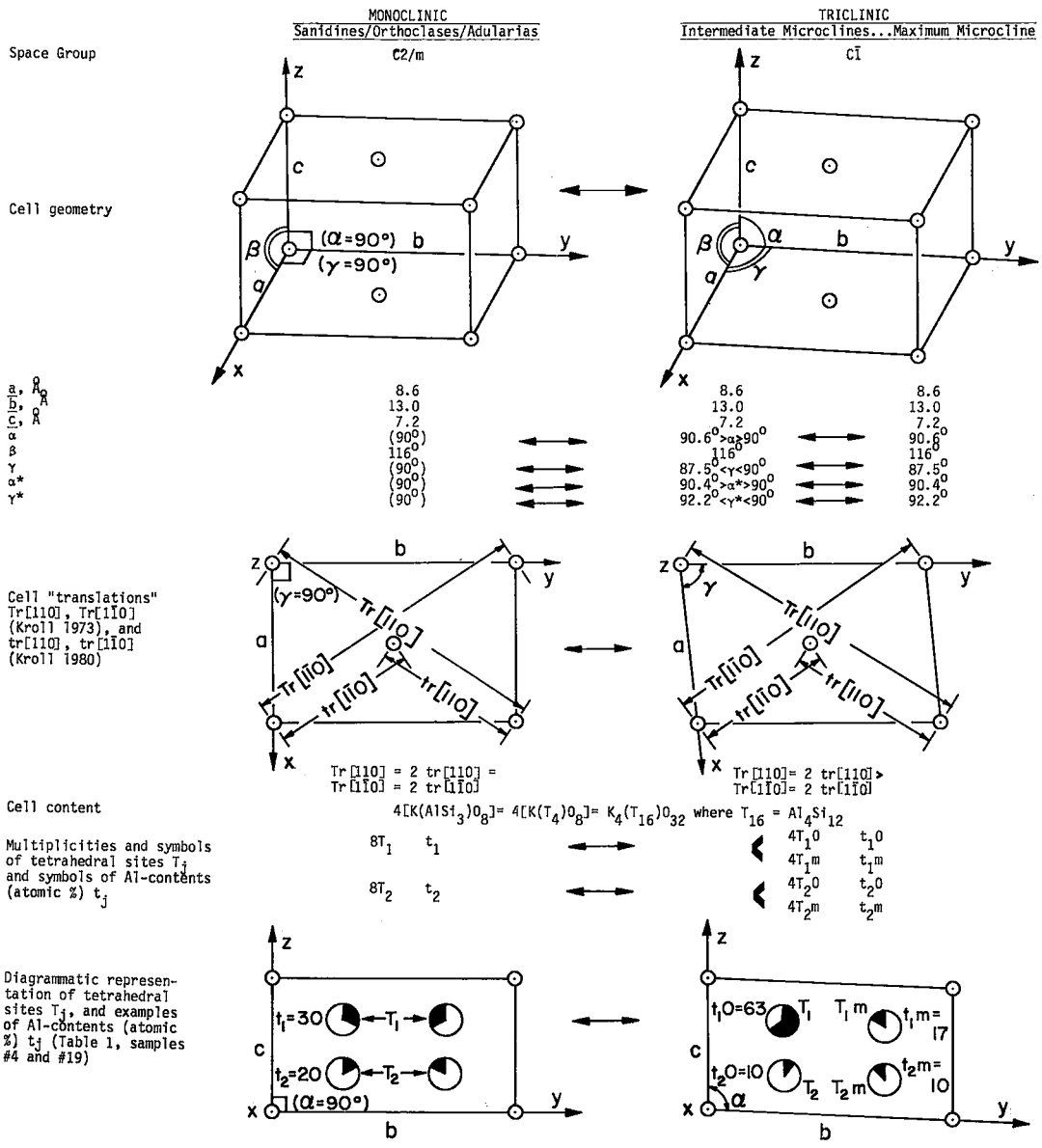

Symbols

⊙ Lattice point

Tj Site ; Solid : % Al tj

Transitional